

Two-dimensional exciton behavior in GaN nanocolumns grown by molecular-beam epitaxy

Jong H. Na, Robert A. Taylor,^{a)} James H. Rice, James W. Robinson, and Kwan H. Lee
Department of Physics, University of Oxford, Parks Road, Oxford OX1 3PU, United Kingdom

Young S. Park, Chang M. Park, and Tae W. Kang
Quantum-functional Semiconductor Research Center, Dongguk University, Seoul 100-715, Korea

(Received 20 September 2004; accepted 30 January 2005; published online 14 March 2005)

We have investigated the behavior of excitons in GaN nanocolumns using time-integrated and time-resolved micro-photoluminescence measurements. In the weak confinement limit, the model of fractional-dimensional space gives an intermediate dimensionality of 2.14 for GaN nanocolumns, with an average diameter of 80 nm. Enhanced exciton and donor binding energies are deduced from a fractional-dimensional model and a phenomenological description. Time-integrated photoluminescence spectra as a function of temperature show a curved emission shift. Recombination dynamics are deduced from the temperature dependence of the PL efficiency and decay times. © 2005 American Institute of Physics. [DOI: 10.1063/1.1885187]

III-nitride semiconductors and their ternary alloys have been investigated intensively because of their great potential in optoelectronic devices in the blue and ultraviolet region of the spectrum.¹ A number of nanostructured nitride-based semiconductor systems have been produced. GaN nanocolumns and quantum discs have been fabricated successfully and confinement effects have been demonstrated.^{2,3} Since many of the properties of excitons depend on dimensionality, an understanding of the role played by confining carriers in such nanoscale systems is desirable. Despite the lateral size of the nanocolumns (~ 200 nm), lateral quantum confinement effects have been observed in ZnMnSe–ZnSe and CdS–ZnS quantum structures.^{4,5} Due to the absence of an appropriate substrate, one of the main issues in GaN is how to reduce the high dislocation density $\sim 10^{10}$ cm⁻². In recent years, self-organized fabrication techniques for nanoscale semiconductors have produced high quality crystals with improved high quantum efficiency and device performance. We present measurement on the dimensionality of, and exciton localization effects in, self-organized GaN nanocolumns with an average diameter of 80 nm.

The GaN nanocolumns studied in this paper were grown by plasma assisted molecular beam epitaxy on Si (111) substrates at 750 °C without any buffer layer.⁶ For time-integrated (TI) and time-resolved (TR) photoluminescence (PL) measurements, frequency-tripled Ti:sapphire laser pulses (~ 100 fs) were used, at a wavelength of 275 nm. A 36 \times reflective objective was held above the cryostat to both focus the incident laser beam and collect the resulting luminescence. The collected luminescence was detected by a CCD mounted on a 0.3 m spectrograph for TI measurements. For TR measurements a commercial time-correlated single photon counting system with a time resolution of 150 ps was used.

The morphology of the nanocolumns is depicted in Fig. 1. The hexagonal GaN nanocolumns exhibit various diameters ranging from 20 to 100 nm, with an average diameter of 80 nm and a density of 2.5×10^8 cm⁻². The columns

studied show different lengths of 2 and 3 μ m, respectively, and the diameter of the columns becomes smaller with increasing height. Although the growth mechanism of columns is based on the Ga balling model,⁷ these compact layer-like coalescence columns at the initial stage of the growth have been observed in AlGaIn nanocolumns introduced by different diffusion coefficients of Al and Ga adatoms. However, the samples used in this paper show coalescence columns despite being pure GaN, implying a different mechanism. Raman spectra show an E_2 high-frequency mode at 568 cm⁻¹, a consequence of strain relaxation of the nanocolumns.

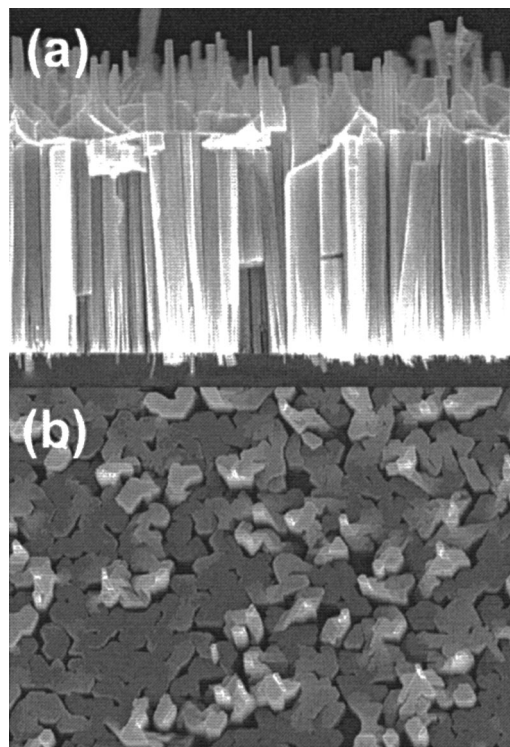


FIG. 1. (a) Cross sectional and (b) plan-view SEM micrographs for GaN nanocolumns with an average diameter of 80 nm and density of 2.5×10^8 cm⁻².

^{a)}Electronic mail: r.taylor1@physics.ox.ac.uk

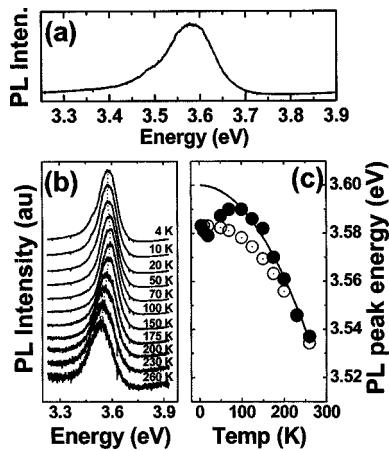


FIG. 2. (a) TI-PL spectrum for a GaN nanocolumn at 4 K. (b) TI-PL spectra for GaN nanocolumns as a function of temperature (4–260 K). (c) TI-PL peak energy as a function of temperature (closed circles) and temperature-induced band-gap shrinkage obtained from Pässler's model (open circles). The solid line is obtained using Vashni fitting, showing good agreement for $T > 100$ K.

Figure 2(a) shows a TI-PL spectrum of GaN nanocolumns recorded at 4 K. The spectrum shows a blue-shifted emission band at 3.583 eV compared to that of three-dimensional (3D) GaN at 3.503 eV.⁸ This occurs even though the diameter of the GaN nanocolumn is larger than the 3D exciton Bohr radius for GaN (~ 11 nm). We have employed a fractional-dimensional model to determine the dimensionality of the nanocolumns.^{9,10} In this model an exciton bound-state energy is given in terms of the degree of dimensionality (α_f) as:

$$E_n = E_g - \frac{\text{Ryd}}{[n + (\alpha_f - 3)/2]^2}.$$

In this equation, E_g and Ryd are the bandgap and 3D exciton Rydberg energy, respectively. Considering the ground-state of the confined exciton ($n=1$), an intermediate dimensionality of 2.14 is obtained, implying that confinement in the nanocolumns is comparable to that in AlGaIn–GaN quantum wells (QWs). The dimensionality of the nanocolumns studied here ranges from 3D (large diameter) to one-dimensional (1D) (smallest diameter) depending on the geometry, with an effective dimensionality of 2.14. The TI-PL spectrum at 4 K is similar to AlGaIn–GaN QWs in terms of the FWHM of the emission bands and the two-dimensional (2D) confinement of carriers, implying that these nanocolumns can be regarded as GaN QWs embedded in a vacuum barrier.

The binding energy E_b of the $1s$ exciton can be estimated using a fractional-dimensional model where the relation to the effective dimensionality is given by:

$$\alpha_f = 1 + 2 \sqrt{\frac{\text{Ryd}}{E_b}}.$$

Substituting Ryd=28 meV, and $\alpha_f=2.14$ (estimated above), we obtain an exciton binding energy of 86.2 meV.

Figure 2(b) shows TI-PL spectra of GaN nanocolumns as a function of temperature. A plot of the peak PL energy versus temperature [Fig. 2(c)] shows a curved shift in energy. A similar shift has been previously observed in multiple quantum wells (MQWs), ternary and binary compound semiconductor films.^{11–14} The shift in emission energy is attributed to

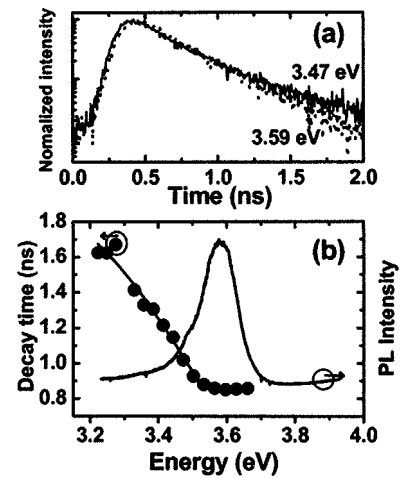


FIG. 3. (a) TR-PL spectra recorded at 4 K at 3.59 and 3.47 eV, showing a biexponential decay trace below 3.5 eV. (b) PL decay time as a function of temperature with TI-PL spectrum at 4 K, and a solid line fitted as mobility edge formalism.

band-tail states arising from layer thickness variation in the limit of MQWs or exciton localization effects due to local potential fluctuation in ternary compound semiconductor films.^{12,15} In the binary compound semiconductor case, the shift can be explained by a thermal release of bound excitons to free excitons, in which the shift of the peak position corresponds to an energy difference between the two.¹⁴ In the case of GaN films, the energy difference of the bound exciton to free exciton transition is ~ 6 meV, implying that the transition temperature would occur at around 70 K.¹² Compared with previous reports, our result is interesting because the GaN nanocolumns are neither ternary alloy semiconductors nor films of GaN.

To compare the shift to temperature dependent bandgap shrinkage of GaN films, we have used Pässler's semiempirical model [plotted in Fig. 2(c)].¹⁶ The experimental peak energies measured at high temperatures are well-described by the Vashni semiempirical model with Vashni fit parameters of $\alpha = 1.6 \times 10^{-3}$ eV/K and $\beta = 1338$ K. From the difference between the low temperature PL maximum and the Vashni plot, the exciton localization energy was evaluated to be 16.8 meV. According to Hayne's rule the donor binding energy is proportional to localization energy with a constant $\alpha = 0.19$ for GaN, implying a donor binding energy of 88.4 meV. However, both values obtained are over three times larger than the 3D exciton Rydberg energy, a consequence of quantum confinement effects. Therefore, in nanocolumns the exciton localization gives rise to an increased exciton binding energy, meaning that the transition from a localized exciton to a free exciton would take place more slowly.

We used TR-PL to study the recombination dynamics of the GaN nanocolumns. Figure 3(a) shows two decay traces recorded at the peak and low-energy side of TI-PL peak. These show that the decay is mono-exponential when monitoring at 3.59 eV and multiexponential at 3.47 eV. Figure 3(b) shows a plot of decay time versus monitoring energy along with a TI-PL spectrum of a nanocolumn as a function of emitted photon energy. The plot shows that as the monitoring energy decreases, the decay time rises from 860 ps to 1.52 ns, where the lifetime is defined as the longer decay component when the decay trace was fitted as a bi-

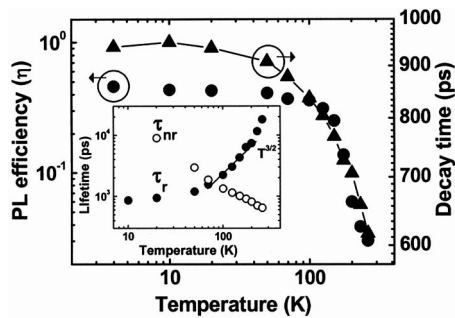


FIG. 4. Temperature dependent PL efficiency (open triangles) and decay time (closed circles). The inset shows radiative and nonradiative lifetimes deduced from PL efficiency and decay time, with a linear increase in radiative lifetime between 100 and ~ 200 K proportional to $T^{3/2}$.

exponential decay. Monoexponential decays were observed for emission energies from 3.66 to 3.5 eV. Bi-exponential decays were evident below 3.5 eV at 4 K with a fast decay component of ~ 250 ps. The weak and broad emission in the TI-PL [Fig. 2(a)] on the low-energy side may originate from coalescent columns (acting as 3D systems) because biexponential decay is seen at energies below 3.5 eV. Its fast decay time of ~ 250 ps is comparable to the D^0X lifetime of 3D-like GaN nanocolumns given in the literature.¹⁷ The longer lived component of the bi-exponential decay seen on the low energy side of the PL peak in Fig. 3(b) may arise from a distribution in the size of the nanocolumns, interface defects between the nanocolumns and the compact layer, or impurities in coalescent columns.

The decay time as a function of emission energy, Fig. 3(b), was fitted using a mobility edge formalism¹⁸

$$\tau = \frac{\tau_r}{1 + \exp[(E_x - E_{me})/E_0]}.$$

The radiative recombination time (τ_r) was estimated at 1.6 ns with a mobility edge energy $E_{me} = 3.49$ eV, and a degree of localization $E_0 = 131$ meV. In contrast to QWs, the E_{me} is lower than the TI-PL peak.^{19,20} To explain this data, we have to consider both coalescence nanocolumns at the bottom of the sample and nanocolumns at the top of the sample, as both can influence PL spectra. The blue-shifted PL peak originated from localized excitons, leading to quantum confinement effects. The low-energy side of the PL is attributed to coalescence nanocolumns. Therefore, the increase in lifetime with decreasing monitoring energy could be ascribed to trapping of the exciton in defect states in the coalescence nanocolumns.

Figure 4 plots the PL efficiency (η) and the decay time as a function of temperature. The PL is expected to be dominated by localized excitons for $T < 100$ K which in turn indicates that τ_r should show a linear increase up to 100 K, typical of 2D free excitons. The decay lifetime is nearly constant for $T < 100$ K, and eventually decreases over 100 K. Delocalization of localized excitons is potentially responsible for the decrease in τ and η . The radiative decay time (τ_r) and nonradiative decay time (τ_{nr}) were deduced from the PL efficiency and decay time as shown the inset of Fig. 4. While τ_{nr} decreases monotonically with temperature, the overall increase in τ_r is close to exponential. There is a very

small variation in τ_r for $T < 100$ K, however, τ_r increases as $T^{3/2}$ between 100 and 200 K due to the decrease in population of excitons or free carriers at $k=0$ with temperature in a bulk semiconductor.²¹ As the temperature further increases, nonradiative annihilation is promoted by dissociation of free excitons into free electrons and holes, giving rise to an increase in τ_r , and reduction in η . Overall, a transition from localized excitons to free excitons is present for $T < 100$ K and free excitons are released thermally into delocalized states in the coalescence columns for $T > 100$ K. These free excitons dissociate into free electrons and holes between 100 and 200 K.

In conclusion, we have observed 2D-like localization effects in GaN nanocolumns grown by MBE. Enhanced binding energies are obtained. An anomaly in the emission shift is attributed to thermal release of localized excitons to free excitons. Compared to GaN/AlGaIn MQWs and GaN films, longer decay time and high quantum efficiency are revealed because of superior crystal quality. For $T < 100$ K, the PL decay time is almost constant due to localization effects. In spite of the increase in τ_r , a sudden decrease in decay times over 100 K is ascribed to thermal release of localized excitons into delocalized states in coalescent columns, giving rise to an increase in the nonradiative annihilation rate of excitons.

The authors would like to acknowledge the support of the KOSEF for funding the QSRC at Dongguk University.

¹F. A. Ponce and D. P. Bour, *Nature (London)* **368**, 351 (1997).

²J. Ristic, E. Calleja, M. A. Sanchez-Garcia, J. M. Ulloa, J. Sanchez-Paramo, J. M. Calleja, U. Jahn, A. Trampert, and K. H. Ploog, *Phys. Rev. B* **68**, 125305 (2003).

³M. Yoshizawa, A. Kikuchi, N. Fujita, K. Kushi, H. Sasamoto, and K. Kishino, *J. Cryst. Growth* **189/190**, 138 (1998).

⁴P. J. Klar, D. Wolverson, and J. J. Davies, *Phys. Rev. B* **57**, 7114 (1998).

⁵F. Gindele, U. Woggon, W. Langbein, J. M. Hvam, M. Hetterich, and C. Klingshirn, *Solid State Commun.* **106**, 653 (1998).

⁶Y. S. Park, C. M. Park, D. J. Fu, T. W. Kang, and J. E. Oh, *Appl. Phys. Lett.* **85**, 5718 (2004).

⁷S. Guha, N. A. Bojarczuk, M. A. L. Johnson, and J. F. Schetzina, *Appl. Phys. Lett.* **75**, 463 (1999).

⁸*Semiconductors-Basic Data* (Springer, Berlin, 1996).

⁹X.-F. He, *Phys. Rev. B* **43**, 2063 (1991).

¹⁰H. Mathieu, P. Lefebvre, and P. Christol, *Phys. Rev. B* **46**, 4092 (1992).

¹¹M. Gallart, A. Morel, T. Taliercio, P. Lefebvre, B. Gil, J. Allegre, H. Mathieu, N. Grandjean, J. Massies, I. Grzegory, and S. Porowsky, *Mater. Sci. Eng.*, **B 82**, 140 (2001).

¹²Y.-H. Cho, G. H. Gainer, J. B. Lam, J. J. Song, W. Yang, and W. Jhe, *Phys. Rev. B* **61**, 7203 (2000).

¹³Y.-H. Cho, G. H. Gainer, A. J. Fischer, J. J. Song, S. Keller, U. K. Mishra, and S. P. DenBaars, *Appl. Phys. Lett.* **73**, 1370 (1998).

¹⁴M. Ichimiya, T. Hayashi, M. Watanabe, T. Ohata, and A. Ishibashi, *Phys. Status Solidi A* **199**, 347 (2003).

¹⁵N. Grandjean, B. Damilano, J. Neu, M. Teissere, I. Grzegory, S. Porowski, M. Gallart, P. Lefebvre, B. Gil, and M. Albrecht, *J. Appl. Phys.* **88**, 183 (2000).

¹⁶R. Passler, *Phys. Status Solidi B* **236**, 710 (2003).

¹⁷E. Calleja, M. A. Sanchez-Garcia, F. J. Sanchez, F. Calle, F. B. Naranjo, E. Munoz, U. Jahn, and K. Ploog, *Phys. Rev. B* **62**, 16826 (2000).

¹⁸C. Gourdon and P. Lavallard, *Phys. Status Solidi B* **153**, 641 (1989).

¹⁹C. K. Choi, Y. H. Kwon, B. D. Little, G. H. Gainer, and J. J. Song, *Phys. Rev. B* **64**, 245339 (2001).

²⁰P. Lefebvre, J. Allegre, B. Gil, A. Kavokine, H. Mathieu, W. Kim, A. Salvador, A. Botchkarev, and H. Morkoc, *Phys. Rev. B* **57**, R9447 (1998).

²¹J. S. Im, A. Moritz, F. Steuber, V. Harle, F. Scholz, and A. Hangleiter, *Appl. Phys. Lett.* **70**, 631 (1996).